Journal of Sustainable Mining 18 (2019) 1–7

HOSTED BY

ELSEVIER

Contents lists available at ScienceDirect

Journal of Sustainable Mining

journal homepage: www.elsevier.com/locate/jsm

Research paper

Analytical design of selected geotechnical solutions which protect civil structures from the effects of underground mining

Rafał Misa*, Anton Sroka, Krzysztof Tajduś, Mateusz Dudek

Strata Mechanics Research Institute, Polish Academy of Sciences, Reymonta 27, 30-059, Cracow, Poland

ARTICLE INFO

Keywords:
Analytical solution
Decompression trench
Geotechnical methods of building protection
Ground surface displacement
Tunnel protection

ABSTRACT

This paper presents the authors' computational methods based on Knothe's theory. The methods enable the estimation of the reduction coefficient for effects which originate from mining operations performed via the application of a longitudinal structure which is sunk in to the ground. It could be, for example, a partition, which as a structural gap fulfils the function of an expansion grout, or via breaking the subsoil continuity (e.g. because of creating a peat-filled ditch or using a natural gap). Demonstrative calculations have been carried out in a few cases, i.a. to protect a structure situated in the vicinity of a planned tunnel. Additionally, some examples of the discontinuity zone which impact the obtained deformation values have been presented. The calculation method has been tested in case studies. The results of the calculations clearly show the positive influence of the applied geotechnical solutions on the minimisation of mining damage.

1. Introduction

This manuscript deals with the problem of underground mining's influence on building structures. The strains in subsidence trough can cause damages to buildings and technical infrastructure (Dai et al., 2010; Florkowska, 2012; Grygierek & Kalisz, 2018; Hegemann, 2018; Hejmanowski & Malinowska, 2016; Jakubowski, Stypulkowski, & Bernardeau, 2017; Karmis, Agioutantis, & Jarosz, 1990; Kowalski & Jędrzejec, 2015; Malinowska, 2017; Peng, 1992; Preusse, Müller, & Beckers, 2018; Rusek, 2017).

Each interference within the rock mass in the form of mining operations leads to changes in its original stress and strain state. This applies also to tunnelling work by means of mining methods, which results in movements of rock and soil, both inside the rock mass and on the ground surface (Migliazzaa, Chiorbolib, & Giania, 2009; Schmidt, 1974; Strokova, 2009). Such movements can frequently result in great, and sometimes disastrous, damage to the building infrastructure (Deck & Singh, 2012; Gayarre, Álvarez-Fernández, González-Nicieza, Álvarez-Vigil, & Herrera Garcíad, 2010; Kwiatek, 2010; Rusek & Firek, 2016). Mining operations are prone to experiencing indirect costs during the execution of works. Damage caused is a direct part of the compensations that mining operators have to provide to third parties, i.e. due to damage in building infrastructure (compensation for the affected communities).

This paper proposes some technical solutions like “a longitudinal structure sunk in the ground, e.g. concrete or steel made of thin-wall sections”, which can prevent damage to the structure of buildings. This paper presents a method of calculating the reduction of strains in the objects protected by those technical prevention solutions.

2. Material and methods

A significant increase in the construction of underground transport workings is a noticeable part of the current development of urban infrastructure (Ilin, Kalinina, Iliashenko, & Levina, 2016; Li & Yeh, 2000; Yigitcanlar & Teriman, 2015). It is anticipated that this trend will continue to increase, both due to the limited land resources on the ground as well as due to the increasing traffic volume.

With such a growing issue, actions aimed at the minimisation of underground mining operations’ impact on the surrounding environment is essential and justifiable. Operations aimed at finding technical solutions, which would enable the effective protection of civil structures against the effects of underground mining have been carried out for many years (Dai, Yang, & Zhao, 1997; Guo, Zhu, Zha, & Wang, 2014; Huang, Zhang, Xu, & Dai, 1996; Luo & Peng, 1991; Zhang et al., 2016). To reduce the impact of construction of, for example, a tunnel on the surface, it seems rational to build a longitudinal structure sunk in to the ground, e.g. concrete or steel made of thin-wall sections. Building

* Corresponding author.
E-mail addresses: misa@img-pan.krakow.pl (R. Misa), sroka@img-pan.krakow.pl (A. Sroka), tajdus@img-pan.krakow.pl (K. Tajduś), dudek@img-pan.krakow.pl (M. Dudek).

https://doi.org/10.1016/j.jsm.2018.10.002
Received 5 July 2018; Received in revised form 8 October 2018; Accepted 28 October 2018
Available online 01 November 2018

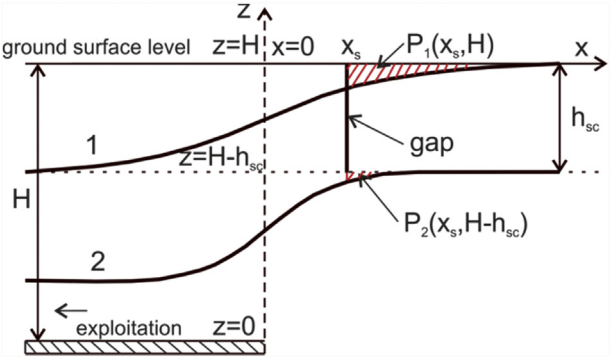

Fig. 1. Rock mass subsidence in the case of mining on the upper (1) and lower (2) level of the gap.

such a structure, referred to as a double partition and named a Trennfuge (structural gap), at some distance from the boundary of mining operations, leads to smaller values of ground subsidence and deformation beyond the partition being obtained as compared to the size of deformations which would occur if such a partition had not been constructed. This structure may protect surface facilities from mining damage (mainly horizontal deformations). Budryk (1954) and Knothe (1954), in fact, suggested such protections during the planning of the metro construction in Warsaw in the 1960s.

2.1. Analytical calculations for mining operations

This article presents a proprietary method to calculate the reduction of deformations in the situation of building a separating partition in an area where mining is being carried out (Sroka, Tajduś, Misa, Hejmanowski, & Florkowska, 2012). An application of an existing method is presented and described. In the case study analysis the shape of mining operations corresponded with the so-called infinite half plane. For the situation presented schematically in Fig. 1, the mean value of reduction coefficient μ_{zm} for the deformation coefficients of land situated beyond the gap (also a natural fissure in the form of an active fault zone) as against the normal course, i.e. without the partition or gap, may be determined according to formula (1) (Sroka et al., 2012).

$$\mu_{zm}(x_s, H, h_{sc}) = \frac{P_2(x_s, H - h_{sc})}{P_1(x_s, H)} \tag{1}$$

where:

μ_{zm} – coefficient of carried out mining impact reduction,
H – depth of mining,
h_{sc} – depth of gap,
x_s – gap situation against the working boundary,
P_2 $(x_s,H\text{-}h_{sc})$ – cross-section area of a subsidence trough situated beyond the gap on the level of its bottom horizon,
P_1 (x_s,H) – cross-section area of a subsidence trough situated beyond point x_s at ground surface level, not considering the gap influence.

The cross-section area of a subsidence trough situated beyond the gap may be calculated according to a general formula:

$$P(x_s, z) = \int_{x_s}^{\infty} w(x, z)\ \mathrm{d}x \tag{2}$$

where:

$w(x, z)$ – course of function describing the subsidence trough profile.

For the gap situated above for the working boundary, i.e. for $x_s = 0$, assuming that the subsidence trough profile is described according to Knothe's theory, we obtain:

$$P_{\max}(x_s = 0, z) = \frac{agr(z)}{2\pi} \tag{3}$$

where:

a – subsidence coefficient,
g – seam thickness,
$r(z)$ – radius of the main influences on any level (z) in the rock mass (for the surface horizon $r(z) = r$ should be assumed).

The value of the main influence's radius is determined according to the following general formulae:

– for $z = H$ (ground surface):

$$r = H \cot\beta \tag{4}$$

– for any position in the rock mass:

$$r(z) = r\left(\frac{z}{H}\right)^n = H^{1-n}z^n \cot\beta \tag{5}$$

where:

β – angle of main influences according to the Knothe definition (1954),
n – coefficient of boundary influence surface, affecting the subsidence trough shape, whose value is within the range of $0.45 \le n \le 0.70$ (Table 1), (Sroka, Knothe, Tajduś, & Misa, 2015).

The formula describing the cross-section area of the subsidence trough can be, assuming that subsidence is described by Knothe's theory, calculated from the formula:

$$P(x_s, z) = P_{\max}(z)\phi\left(\frac{x_s}{r(z)}\right) \tag{6}$$

Values of function ϕ calculated numerically for $\frac{x}{r(z)}$ every 0.05 are presented in Fig. 2 and in Table 2.

Moving to the reduction coefficient and substituting (3) to (6), and then substituting the obtained equation to formula (1), we obtain:

$$\mu_{zm}(x_s, H, h_{sc}) = \frac{P_2(x_s, H - h_{sc})}{P_1(x_s, H)} = \frac{\frac{agr(z)}{2\pi}\phi\left(\frac{x_s}{r(z)}\right)}{\frac{agr}{2\pi}\phi\left(\frac{x_s}{r}\right)} = \frac{r(z)}{r}\frac{\phi\left(\frac{x_s}{r(z)}\right)}{\phi\left(\frac{x_s}{r}\right)} < 1 \tag{7}$$

Values of ratio $\frac{r(z)}{r} = \left(\frac{z}{H}\right)^n = \left(\frac{H-h_{sc}}{H}\right)^n = \left(1 - \frac{h_{sc}}{H}\right)^n$, and of ratio $\frac{\phi\left(\frac{x_s}{r(z)}\right)}{\phi\left(\frac{x_s}{r}\right)}$ are less than 1.0.

Table 1
Value of coefficient n depending on various hypotheses.

Author	Year	Value
Budryk	1953	$n = \sqrt{2\pi}\tan\beta$
Mohr[a]	1958	$n = 0.65$
Krzysztoń	1965	$n = 1.0$
Drzęźla[a]	1972	$n = 0.525$
Sroka, Bartosik-Sroka	1974	$n = 0.50$
Drzęźla	1975	$n = 0.665$
Gromysz[a]	1977	$n = 0.61$
Drzęźla[a]	1979	$0.47 \le n \le 0.49$
Kowalski[a]	1984	$0.48 \le n \le 0.66$
Drzęźla[a]	1989	$0.45 \le n \le 0.70$
Preusse[a]	1990	$n = 0.54$

[a] Papers provide values of coefficient n determined based on *in situ* measurement results.

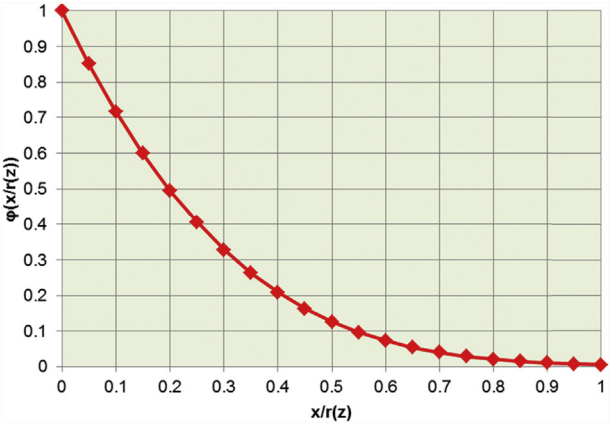

Fig. 2. Calculated values of function ϕ for $x/r(z)$.

Table 2
Table of function $\phi\left(\frac{x}{r(z)}\right)$.

$x/r(z)$	$\varphi(x/r(z))$	$x/r(z)$	$\varphi\ (x/r(z))$	$x/r(z)$	$\varphi\ (x/r(z))$
0.00	1.0000	0.35	0.2629	0.70	0.0403
0.05	0.8510	0.40	0.2083	0.75	0.0294
0.10	0.7174	0.45	0.1632	0.80	0.0211
0.15	0.5991	0.50	0.1263	0.85	0.0150
0.20	0.4953	0.55	0.0967	0.90	0.0105
0.25	0.4053	0.60	0.0731	0.95	0.0073
0.30	0.3282	0.65	0.0546	1.00	0.0050

Both values show the influence of the gap depth and the influence of its position in relation to the working boundary on the average value of reduction coefficients of deformation coefficients for the land situated beyond the gap.

2.2. Methods of the protection of civil structures

As shown by in-situ observations, the application of a tight partition or breaking the subsoil continuity (e.g. due to making a ditch filled with peat) results in reducing the influence impact beyond the partition (Fig. 3), where line *A* marks the influence behind the partition and line *B* the influence without it.

At the gap edge there is discontinuous distribution of deformation at point x_s. This can be observed by a disturbed subsidence distribution and varying gap width. In the case of installing (performing) geotechnical protection in the form of a "gap" (partition), the distribution of subsidence behind the partition is described by:

$$w_s(x > x_s) = w(x > x_s)\mu_{zm}(x_s, h_{sc}) \tag{8}$$

where:

$w_s(x > x_s)$ – subsidence behind the partition,
$w(x > x_s)$ – subsidence without the partition,
μ_{zm} – coefficient of impact reduction depending on the partition's position in relation to the tunnel axis and to the partition depth,
x_s – coordinate of the partition's position in relation to the tunnel axis,
h_{sc} – depth of partition driving.

The reduction coefficient μ_{zm} is defined by means of a general formula (1).

Assuming that the ground surface subsidence is described by (9) (Hörich & Sroka, 2004):

$$w(x) = w_0 \exp\left(-\pi\frac{x^2}{r^2}\right) \tag{9}$$

where: $w_0 = \frac{\Delta F}{r}$,

w_0 – subsidence above the tunnel's vertical axis,
ΔF – convergence of the working (tunnel) in the sense of cross-section reduction, $\Delta F = \lambda_K F$, where λ_K is a relative convergence coefficient; according to Peck (1969) its value ranges from around 1% to a maximum of 3%,

we obtain:

$$P(x_s) = \int_{x_s}^{\infty} w(x)\,\mathrm{d}x = \frac{\Delta F}{r}\int_{x_s}^{\infty} \exp\left(-\pi\frac{x^2}{r^2}\right)\mathrm{d}x \tag{10}$$

and finally:

$$P(x_s) = \Delta F\int_{x_s/r}^{\infty} \exp(-\pi\xi^2)\,\mathrm{d}\xi = \Delta F Y\left(\frac{x_s}{r}\right) \tag{11}$$

Function $Y\left(\frac{x_s}{r}\right)$ may be described by an approximate formula (Sroka et al., 2012):

$$Y\left(\frac{x_s}{r}\right) = 0.5\exp\left\{-1.22\left(\frac{x_s}{r}\right)\left[2\left(\frac{x_s}{r}\right) + 1.57\right]\right\}. \tag{12}$$

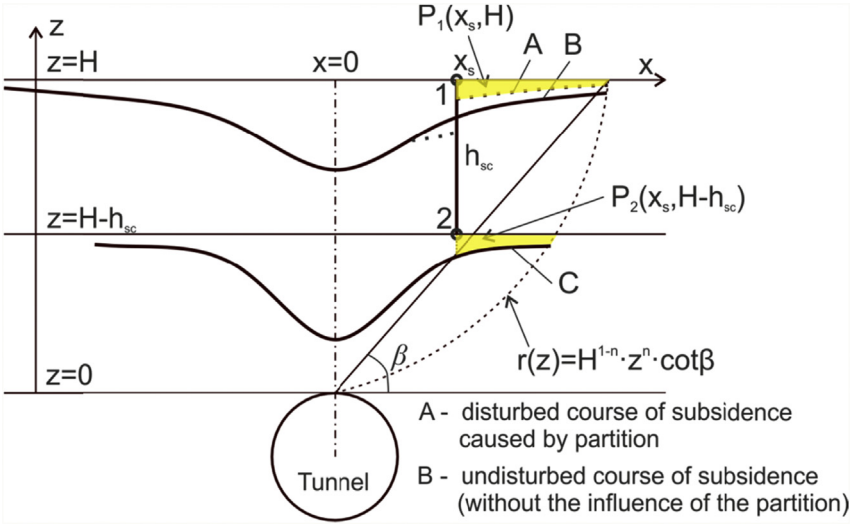

Fig. 3. Rock mass subsidence on the level of partition foot *(C)* and subsidence of the surface without the partition *(B)* and beyond the partition, if driven *(A)*.

Table 3
Table of function $Y\left(\frac{x_s}{r}\right)$, described by an accurate formula (Knothe, 1984).

x_s/r	$Y(x_s/r)$	x_s/r	$Y(x_s/r)$	x_s/r	$Y(x_s/r)$
0.00	0.5000	0.45	0.1297	0.90	0.0120
0.05	0.4501	0.50	0.1050	0.95	0.0086
0.10	0.4010	0.55	0.0840	1.00	0.0061
0.15	0.3535	0.60	0.0663	1.10	0.0029
0.20	0.3080	0.65	0.0516	1.20	0.0013
0.25	0.2654	0.70	0.0397	1.30	0.0006
0.30	0.2260	0.75	0.0300	1.40	0.0002
0.35	0.1902	0.80	0.0225	1.50	0.0001
0.40	0.1580	0.85	0.0166	1.60	0.00003

Values of function $Y\left(\frac{x_s}{r}\right)$ described by an accurate formula are presented in Table 3.

When considering upper $P_1(x_s, H)$ and lower $P_2(x_s, H\text{-}h_{sc})$ point of tight partition (Fig. 3) we obtain:

$$P_1(x_s, H) = \Delta FY\left(\frac{x_s}{r_1}\right) \tag{13}$$

$$P_2(x_s, H - h_{sc}) = \Delta FY\left(\frac{x_s}{r_2}\right) \tag{14}$$

and as a result:

$$\mu(x_s, h_{sc}) = \frac{Y\left(\frac{x_s}{r_1}\right)}{Y\left(\frac{x_s}{r_2}\right)} \tag{15}$$

where:

$$r_1 = r = H \cot\beta \tag{16}$$

$$r_2 = r\left(\frac{H - h_{sc}}{H}\right)^n = r\left(1 - \frac{h_{sc}}{H}\right)^n \tag{17}$$

h_{sc} – effective depth of partition.

3. Results of the research

3.1. Estimation of the influence of the discontinuity zone on the course of deformation – examples

As experience and *in situ* observations have shown, a gap may be understood also as natural tectonic disturbances existing in rock mass, e.g. faults, which in the past resulted in numerous discontinuous deformations on the surface. In this case the overburden layer's thickness should be taken as the depth of the gap.

To illustrate the gap influence on the distribution of deformation coefficients in the ground tension zone situated beyond the gap, a theoretical example was analysed and the following data was assumed in relation to the natural gap position and depth, in addition to data related to the planned mining operations:

- parameters characterising the fault:
  $x = 100$ m, $H = 700$ m, $h_{sc} = 150$ m,
- parameters characterising the rock mass quality:
  $n = 0.5$, $\beta = 63.4^\circ$.

The value of the radius of the main influence on the ground surface is: $r_1 = r = H \cot\beta = 351$ m. The ratio of the gap distance from the working boundary to the value of the radius of the main influence for the ground surface is: $\frac{x_s}{r_1} = 0.285 \approx 0.29$. Using Table 2, by means of interpolation, we obtain $\phi\left(\frac{x_s}{r_1}\right) = 0.3509$.

For the lower limit of the gap we obtain the following results: $z = H - h_{sc} = 550$ m. To calculate the value of the radius of the main influence we assume that the value of the boundary surface coefficient is $n = 0.5$ and we obtain:

$$r_2 = r\left(\frac{z}{H}\right)^n = 310.7 \text{ m}.$$

The ratio of the gap distance from the working boundary to the value of the radius of the main influence inside the rock mass is:

$$\frac{x_s}{r_2} = \frac{100}{310.7} = 0.322 \approx 0.32.$$

Using values presented in Table 2, by means of interpolation, we obtain $\phi\left(\frac{x_s}{r_2}\right) = 0.2997$.

The value of reduction coefficient is therefore:

$$\mu_{zm}(x_s, h_{sc}) = \frac{r_2}{r_1}\frac{\phi\left(\frac{x_s}{r_2}\right)}{\phi\left(\frac{x_s}{r_1}\right)} = \frac{310.7}{350.5}\frac{0.2997}{0.3509} = 0.7571$$

which results in approximately a 1.3 times reduction of the mining impact as compared with the normal course (not disturbed by a natural gap).

A detailed example, using the actual data, is presented below. On the basis of geodetic-geological data presented by Tyrała (1979), calculations were performed for the mining of longwall no. 120 in seam 414a of the Dymitrow coalmine (current name: Bobrek Centrum), situated at the depth of $H = 470$ m. The mining has been carried out close to a normal longitudinal fault, with inclination opposite to the direction of the mining front. Fig. 4 presents the location of measuring points (observation line + scattered points) against the panel and the fault.

The following values of parameters were used for calculations:

- parameters characterising the fault:
  $x_{s1} = 50$ m, $x_{s2} = 100$ m, $h_{sc} = 300$ m,
- parameters characterising the rock mass quality:
  $n = 0.5$, $\beta = 63.4^\circ$.

The value of the radius of the main influence for the ground surface is: $r_1 = 235.4$ m. For the first case ($x_{s1} = 50$ m) the ratio of the gap

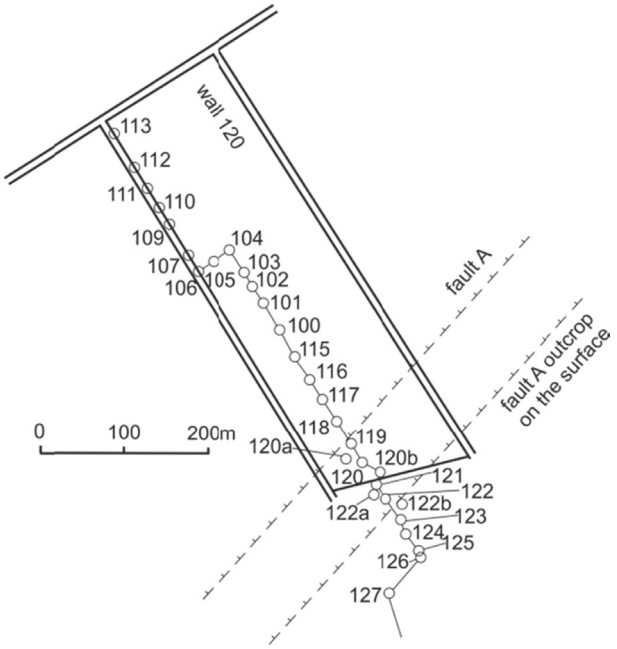

Fig. 4. Mutual situation of the mine working, observation line and fault 'A' (Tyrała, 1979).

distance from the working boundary to the value of the radius of the main influence for the ground surface is: $\frac{x_{s1}}{r_1} = 0.212 \approx 0.21$. Using Table 2, by means of interpolation, we will obtain the value of the function for the specific ratio $\frac{x_{s1}}{r_1}$ and it is: $\varphi\left(\frac{x_{s1}}{r_1}\right) = 0.4729$. For the second case ($x_{s1} = 100$ m) the function value will be: $\frac{x_{s2}}{r_1} = 0.425 \approx 0.43$ and $\varphi\left(\frac{x_{s2}}{r_1}\right) = 0.1859$.

Further calculations were carried out for the lower boundary of the fault, i.e. for the vertical distance: $z = H - h_{sc} = 170$ m, assuming the value of the boundary surface coefficient to be $n = 0.5$. The following were obtained for such assumptions: $r_2 = r\left(\frac{z}{H}\right)^n = 141.6$ m. , and then for both cases the following values were obtained:

$$\frac{x_{s1}}{r_2} = \frac{50}{141.6} = 0.353 \approx 0.35 \text{ and } \frac{x_{s2}}{r_2} = \frac{100}{141.6} = 0.706 \approx 0.71.$$

Using the values presented in Table 2, by means of interpolation, the following were obtained:

$$\varphi\left(\frac{x_{s1}}{r_2}\right) = 0.2594 \text{ and } \left(\frac{x_{s2}}{r_2}\right) = 0.0389.$$

Finally, the value of the reduction coefficient for two cases is:

$$\mu_{zm}(x_{s1}, h_{sc}) = \frac{141.6}{235.4}\frac{0.2594}{0.4729} = 0.3299 \text{ and } \mu_{zm}(x_{s2}, h_{sc}) = \frac{141.6}{235.4}\frac{0.0389}{0.1859} = 0.1258$$

which results in approximately a 3 times reduction in the mining impact as compared with the normal course (not disturbed by a natural gap) for the first case and an almost 8 times reduction in the impact for the second case.

3.2. Blocking wall in the vicinity of a planned tunnel – a computational example

The presented example concerns a situation in which a partition was driven in the vicinity of the underground tunnelling which had been carried out, where the tunnel has the shape of a circle with a radius $R_T = 4$ m, is situated at the depth of $H = 30$ m and the partition distance from the tunnel axis is $x_s = 12$ m (Fig. 3). In addition, the overburden features properties which correspond to the adoption of the following parameter values: $\beta = 45^\circ$, $n = 0.5$ and the tunnel convergence coefficient $\lambda_K = 1.5\%$ ($\Delta F = 0.75\ m^2$).

Calculations were carried out using an approximate formula (12). Two cases were considered, in the first the partition depth was $h_{sc1} = 16.7$ m, and in the second $h_{sc2} = 10.8$ m. The course and results of the calculations are presented in Table 4.

The results show that if a partition is driven to a depth of 16.7 m, the tunnel impact for $x > x_s$ ($x > 12$ m) will be reduced by approximately 2.4 times when compared to the impact which would occur without the partition application, while for the partition which is 10.8 m deep the impact will be reduced by 1.5 times (in the area beyond the partition).

4. Discussion

The above examples confirm that the nature of natural gaps' behaviour and their impact on the surface is similar to cases which use decompression ditches. In both cases differences in deformation values "before and behind" the gap/ditch are observed. When comparing the measured deformation coefficients with theoretically calculated coefficients (Fig. 5), following Tyrała (1979), it is possible to notice that:

- the right-hand side of the profile, belonging to the subsidence trough was shortened, (it is visible that the impact is not transferred beyond the fault),
- the disturbances covered the section of the subsidence trough profile between points 118–126; the disturbances are most visible in the

Table 4
Calculations of ground surface deformation reduction for the driven tunnel.

Calculations for $h_{sc1} = 16.7$ m:		Calculations for $h_{sc2} = 10.8$ m:
Point (1)	$r_1 = r = H\cot\beta = 30\ \text{m}\frac{x_s}{r_1} = \frac{12}{30} = 0.40Y\left(\frac{x_s}{r_1} = 0.40\right) = 0.1580$	Point (1)	$r_1 = r = H\cot\beta = 30m\frac{x_s}{r_1} = \frac{12}{30} = 0.40Y\left(\frac{x_s}{r_1} = 0.40\right) = 0.1580$
Point (2)	$z_1 = H - h_{sc1} = 13.3\ \text{m}r_2 = r\left(\frac{z1}{H}\right)^n = 19.97\ \text{m}\frac{x_s}{r_2} = \frac{12}{19.97} = 0.60Y\left(\frac{x_s}{r_2} = 0.60\right) = 0.0663$	Point (2)	$z_2 = H - h_{sc2} = 19.2mr_2 = r\left(\frac{z2}{H}\right)^n = 24.0\ \text{m}\frac{x_s}{r_2} = \frac{12}{24.0} = 0.50Y\left(\frac{x_s}{r_2} = 0.50\right) = 0.1050$
Value of deformation reduction coefficient			
$\mu(x_s, h_{sc}) = \frac{Y\left(\frac{x_s}{r_1}\right)}{Y\left(\frac{x_s}{r_2}\right)} = \frac{0.0663}{0.1580} = 0.4196$		$\mu_{zm}(x_s, h_{sc}) = \frac{Y\left(\frac{x_s}{r_1}\right)}{Y\left(\frac{x_s}{r_2}\right)} = \frac{0.1050}{0.1580} = 0.6646$	

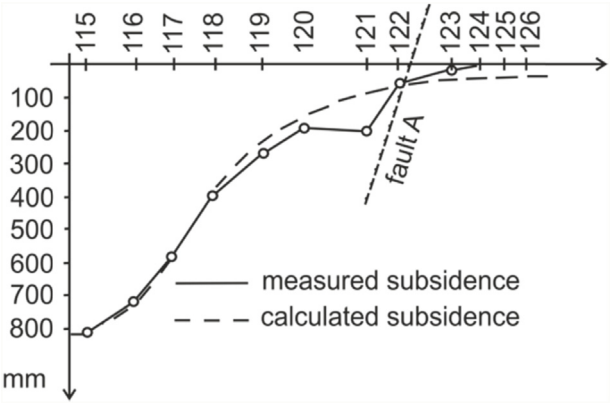

Fig. 5. Comparison of measured and calculated subsidence (Tyrała, 1979).

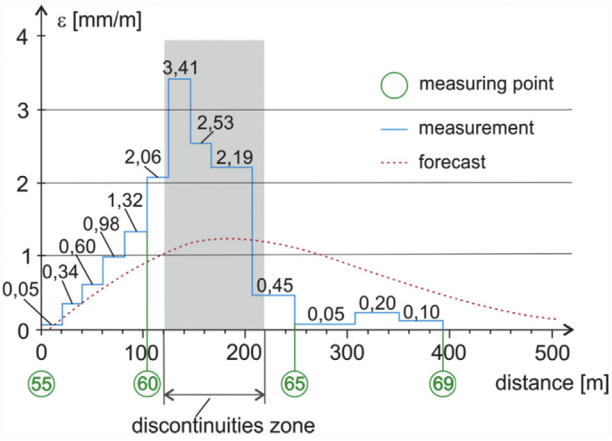

Fig. 6. The discontinuity zone's impact on the deformation values in the Niederberg mine (Geitling 2 seam) (Grün, 1995).

vicinity of point 121 situated at the fault fissure outcrop,
– towards point 126 the measured subsidence clearly decreases when compared to the forecast values.

Grün (1995), while analysing the data from the Niederberg mine for seam Geitling 2, presented an example of the discontinuity zone's impact on the results of obtained deformations. In the zone of existing discontinuities (Fig. 6) the deformation values exceeded 2 mm/m and were much higher than the forecasted values (the broken line). It is noticeable in Fig. 6 that in around a 100-m zone of discontinuities the deformations cumulated and outside this zone (to the right hand side) there are practically no deformations. A similar effect (deformation reduction) is observed when looking at a geotechnical ditch protecting a civil structure.

Tectonic faults are not a single surface, but a system of many surfaces. They create a fault zone, whose width can reach a few dozen millimetres. From the mining operation point of view, tectonic faults are an element which limits mining operations. At the excavation of many seams in the fault zone the tensile deformations sum up, which can result and – as shown by the mining practice – do result in releasing such zones. They then create “a structural gap” in the rock mass, which transfers only part of the mining impact. However, this “protective impact” results in the occurrence of discontinuous deformations in the fault zone outcrop on the surface. In numerous cases this is a “protective” action used in planning the mining operations in terms of their impact minimisation.

The methodology of proceeding, suggested by Sroka (2008), using the symmetry of the horizontal displacement course disturbance and subsidence, caused by the gap, is an example of such a solution. Using the formulated mathematical model, the threshold heights created (Δw) or the width of the formed gaps (Δu) may be determined according to (18) and (19) (Sroka, 2008):

$$\text{threshold height: } \Delta w(x_s) = 2(1-\mu)w(x_s) \tag{18}$$

$$\text{gap width: } \Delta u(x_s) = 2(1-\mu)u(x_s) \tag{19}$$

where:

μ – coefficient (based on observations μ = 0.10–0.15 can be taken),
$w(x)$ – subsidence values,
$u(x)$ – horizontal displacement value (without the fault fissure).

5. Conclusions

The idea of geotechnical protections consists of separating the civil structure from the deformed subsoil (Misa, 2016). The use of this idea enabled the present analytical computations by means of a proprietary method. According to the considerations in the case of the analysis of partition impact on the surrounding ground, the partition effectiveness depends on its position in relation to the tunnel axis and on its depth.

Both for the situation of natural gaps existing in the soil and for the performance of partitions in the vicinity of a tunnel, the reduction of deformation values and subsoil displacements is higher when using geotechnical protection of greater depth. The effectiveness of such solutions has been confirmed by the calculation examples presented. In his doctoral thesis Misa (2016), carrying out numerical computations, fully confirmed the applicability of the analytical solutions presented in this paper.

Conflicts of interest

None declared.

Ethical statement

The authors state that the research was conducted according to ethical standards.

Funding

None.

Appendix A. Supplementary data

Supplementary data to this article can be found online at https://doi.org/10.1016/j.jsm.2018.10.002.

References

Budryk, W. (1954). Wpływ niektórych konstrukcji budowlanych na przemieszczenia i odkształcenia powierzchni [The influence of some building structures on surface displacement and deformation]. *Archiwum Gornictwa i Hutnictwa, 2*(4), 423–445.

Dai, H., Lian, X., Liu, J., Liu, Y., Zhou, Y., Deng, W., et al. (2010). Model study of deformation induced by fully mechanized caving below a thick loess layer. *International Journal of Rock Mechanics and Mining Sciences, 47*(6), 1027–1033. https://doi.org/10.1016/j.ijrmms.2010.06.005.

Dai, H., Yang, G., & Zhao, Q. (1997). Building artificial weak plane protection method and its application research. *Mining Survey, 5*(2), 14–17. (in Chinese) http://www.doc88.com/p-5045696832581.html.

Deck, O., & Singh, A. (2012). Analytical model for the prediction of building deflections induced by ground movements. *International Journal for Numerical and Analytical Methods in Geomechanics, 36*(1), 62–84. https://doi.org/10.1002/nag.993.

Florkowska, L. (2012). Building protection against the backdrop of current situation and growth perspectives for the Polish mining industry. *Archives of Mining Sciences, 57*(3), 645–655. https://doi.org/10.2478/v10267-012-0041-2.

Gayarre, L., Álvarez-Fernández, M. I., González-Nicieza, C., Álvarez-Vigil, A. E., & Herrera Garcíad, G. (2010). Forensic analysis of buildings affected by mining subsidence. *Engineering Failure Analysis, 17*(1), 270–285. https://doi.org/10.1016/j.engfailanal.2009.06.008.

Grün, E. (1995). *Analyse und Prognose von Unstetigkeiten als Folge bergbaubedingter*

Bodenbewegungen im Linksniederrheinischen Steinkohlengebiet [Analysis and prognosis of discontinuities as a result of mining-related ground movements in the Lower Rhine coal area](PhD thesis). Aachen, Germany: Rheinisch-Westfalische Technische Hochschule (RWTH).

Grygierek, M., & Kalisz, P. (2018). Influence of mining operations on road pavement and sewer system – selected case studies. *Journal of Sustainable Mining, 17*(2), 56–67. https://doi.org/10.1016/j.jsm.2018.04.001.

Guo, G., Zhu, X., Zha, J., & Wang, Q. (2014). Subsidence prediction method based on equivalent mining height theory for solid backfilling mining. *Transactions of Nonferrous Metals Society of China, 24*(10), 3302–3308. https://doi.org/10.1016/S1003-6326(14)63470-1.

Hegemann, M. (2018). Scientific importance of the academic achievements of professor Knothe for ground movement calculation in Germany. *Prace Instytutu Mechaniki Górotworu PAN, 20*(1), 33–44. http://www.img-pan.krakow.pl/index.php/en/component/docman/doc_download/647-201801-04-hegemann.html.

Hejmanowski, R., & Malinowska, A. A. (2016). Significance of the uncertainty level for the modelling of ground deformation ranges. *International Journal of Rock Mechanics and Mining Sciences, 83*, 140–148. https://doi.org/10.1016/j.ijrmms.2015.12.019.

Hörich, S., & Sroka, A. (2004). Vorausberechnung der Bodenbewegungselemente über Tunnelbauten im Lockergebige [Prediction of the ground movement elements over tunnels in the Lockered]. *Proceedings of XII international congress of international society for mine surveying, Fuxin-Beijing, China, 20–26.09.2004* (pp. 528–531). (Beijing).

Huang, L., Zhang, J., Xu, J., & Dai, H. (1996). Research on indirect protection technology of foundation rock in a mining area. *Coal Science and Technology, 2*(2), 2–7. (in Chinese). Retrieved July 14, 2018, from http://www.doc88.com/p-1167434341355.html.

Ilin, I., Kalinina, O., Iliashenko, O., & Levina, A. (2016). Sustainable urban development as a driver of safety system development of the urban underground. *Procedia Engineering, 165*, 1673–1682. https://doi.org/10.1016/j.proeng.2016.11.909.

Jakubowski, J., Stypulkowski, J. B., & Bernardeau, F. G. (2017). Multivariate linear regression and cart regression analysis of TBM performance at Abu Hamour phase-I tunnel. *Archives of Mining Sciences, 62*(4), 825–841. https://doi.org/10.1515/amsc-2017-0057.

Karmis, M., Agioutantis, Z., & Jarosz, A. (1990). Recent developments in the application of the influence function method for ground movement predictions in the U.S. *Mining Science and Technology, 10*(3), 233–245. https://doi.org/10.1016/0167-9031(90)90439-Y.

Knothe, S. (1954). Przybliżona metoda wyznaczania wielkości odkształceń powierzchni poza ścianką zaporową [An approximate method for determining the magnitude of surface deformation outside the retaining wall]. *Archiwum Gornictwa i Hutnictwa, 2*(4), 473–487.

Knothe, S. (1984). *Prognozowanie wpływów eksploatacji górniczej [Forecasting the impact of mining operations* (1st ed.). Katowice: Wydawnictwo Śląsk.

Kowalski, A., & Jędrzejec, E. (2015). Influence of subsidence fluctuation on the determination of mining area curvatures. *Archives of Mining Sciences, 60*(2), 487–505. https://doi.org/10.1515/amsc-2015-0032.

Kwiatek, J. (2010). Fault diagnosis of building structures in mining areas. *Archives of Mining Sciences, 55*(2), 313–330.

Li, X., & Yeh, A. G.-O. (2000). Modelling sustainable urban development by the integration of constrained cellular automata and GIS. *International Journal of Geographical Information Science, 14*(2), 131–152. https://doi.org/10.1080/136588100240886.

Luo, Y., & Peng, S. S. (1991). Protecting a subsidence affected house: A case study. *Proceedings of the VIII congress international society for mine surveying, Kentucky, USA* (pp. 297–300). (Kentucky).

Malinowska, A. A. (2017). Fuzzy inference-based approach to the mining-induced pipeline failure estimation. *Natural Hazards, 85*(1), 621–636. https://doi.org/10.1007/s11069-016-2594-4.

Migliazzaa, M., Chiorbolib, M., & Giania, G. P. (2009). Comparison of analytical method, 3D finite element model with experimental subsidence measurements resulting from the extension of the Milan underground. *Computers and Geotechnics, 36*(1–2), 113–124. https://doi.org/10.1016/j.compgeo.2008.03.005.

Misa, R. (2016). Metody ograniczenia wpływu eksploatacji podziemnej na obiekty budowlane poprzez zastosowanie rozwiązań geotechnicznych [Geotechnical solutions as the methods for reducing the impact of underground mining exploitation on construction]. *Prace Instytutu Mechaniki Górotworu PAN*. Kraków: Instytut Mechaniki Górotworu PAN.

Peck, R. B. (1969). Deep excavations and tunneling in soft ground. *7th international conference on soil mechanics and foundation engineering: Vol. 7*, (pp. 225–290). (3).

Peng, S. S. (1992). *Surface subsidence engineering.* Littleton, CO: Society for Mining, Metallurgy, and Exploration.

Preusse, A., Müller, D., & Beckers, D. (2018). Challenges in German subsidence research – retrospectives and perspectives. *Prace Instytutu Mechaniki Górotworu PAN, 20*(1), 25–32. Retrieved July 14, 2018, from http://www.img-pan.krakow.pl/index.php/en/component/docman/doc_download/648-201801-04-preusse.html.

Rusek, J. (2017). Application of support vector machine in the analysis of the technical state of development in the LGOM mining area. *Eksploatacja i Niezawodność – Maintenance and Reliability, 19*(1), 54–61. https://doi.org/10.17531/ein.2017.1.8.

Rusek, J., & Firek, K. (2016). Assessment of technical condition of prefabricated large-block building structures located in mining area using the naive bayes classifier. *16th international multidisciplinary scientific GeoConference SGEM 2016, SGEM2016 conference proceedings: Vol. 2*, (pp. 109–116). . https://doi.org/10.5593/SGEM2016/B52/S20.015 Book 5.

Schmidt, B. (1974). Prediction of settlements due to tunnelling in soil: Three case histories. In: *Proc. 2nd rapid excavation tunnelling conference, San Francisco, CA* (pp. 1179–1199). (San Francisco).

Sroka, A. (2008). Designing coal extraction where the surface is threatened by discontinuous linear deformations. *Gospodarka Surowcami Mineralnymi-Mineral Resources Management, 24*(2/3), 445–455.

Sroka, A., Knothe, S., Tajduś, K., & Misa, R. (2015). Underground exploitations inside safety pillar shafts when considering the effective use of a coal deposit. *Gospodarka Surowcami Mineralnymi-Mineral Resources Management, 31*(3), 93–110. https://doi.org/10.1515/gospo-2015-0027.

Sroka, A., Tajduś, K., Misa, R., Hejmanowski, R., & Florkowska, L. (2012). *Wykorzystanie metod geotechnicznych w celu ograniczenia wpływów eksploatacji podziemnej na obiekty budowlane [Use of geotechnical methods to reduce the impact of underground mining on buildings]. Research Report No. N N524 466636*Cracow, Poland: Laboratory of Rock Deformation, Strata Mechanics Research Institute of the Polish Academy of Sciences.

Strokova, L. A. (2009). Numerical model of surface subsidence during subway tunnelling. *Soil Mechanics and Foundation Engineering, 46*(3), 117–119. https://doi.org/10.1007/s11204-009-9050-3.

Tyrała, A. (1979). *Wpływ uskoków tektonicznych na zaburzenia obniżeń powierzchni wywołanych przez eksploatację górniczą [The influence of tectonic faults on disturbances of surface subsidence caused by mining exploitation] (PhD thesis)*Katowice, Poland: Główny Instytut Górnictwa.

Yigitcanlar, T., & Teriman, S. (2015). Rethinking sustainable urban development: Towards an integrated planning and development process. *International Journal of Environmental Science and Technology, 12*(1), 341–352. https://doi.org/10.1007/s13762-013-0491-x.

Zhang, P., Peterson, S., Neilans, D., Wade, S., McGrady, R., & Pugh, J. (2016). Geotechnical risk management to prevent coal outburst in room-and-pillar mining. *International Journal of Mining Science and Technology, 26*(1), 9–18. https://doi.org/10.1016/j.ijmst.2015.11.003.